Korean J. Chem. Eng., **26**(3), 770-774 (2009)

Physical and electrochemical properties of lithium-doped 1-butyl-3-methylimidazolium salts

Ki-Sub Kim†

Department of Chemical and Biological Engineering, Chungju National University,
72, Daehak-ro, Chungju, Chungbuk 380-702, Korea
(*Received 30 June 2008 • accepted 12 December 2008*)

Abstract−Two well known room temperature ionic liquids (RTILs), 1-butyl-3-methylimidazolium tetrafluoroborate ([BMIm][BF_4]) and 1-butyl-3-methylimidazolium iodide ([BMIm][I]), were synthesized. Their physical properties such as reflective indices, densities, viscosities, heat capacities, and heats of dilution were measured. The overall properties of [BMIm][BF_4] obtained after two-step reactions were superior to those of the IL with a halide anion. The incorporation of lithium ions using lithium tetrafluoroborate ($LiBF_4$) in each IL was carried out and ionic conductivities as a function of temperature and Li ion concentration were investigated. The isothermal conductivity graph showed a parabolic curve shape suggesting that the maximum values exist at a specific concentration condition while they continuously increased as the temperature increased. The conductivities reached as high as 10^{-3} $S \cdot cm^{-1}$.

Key words: Physical Properties, Electrochemical Properties, Ionic Liquid, Li-doped Ionic Liquids

INTRODUCTION

It is well known that ionic liquids (ILs) are environmentally benign solvents because they have very low vapor pressure and are stable in a wide temperature range. They generally feature good stability in air and water, a wide liquid range, and relatively favorable viscosity and density characteristics. Moreover, either the length of the side chain of their cation or their specifically designed anion can be easily controlled for various uses [1-3]. These characteristics also contribute to their application to different types of electrolytes for use in electrochemical systems [4-15]. MacFarlane and Forsyth developed various electrolyte systems based on ILs such as plastic crystalline and IL-polymer electrolytes, opening a new field of lithium-doped ILs exhibiting fast Li-ion conduction [4-10]. In our previous work, we developed new IL electrolytes which were based on morpholinium salts [11-15]. The morpholinium ILs have the advantages of easy synthesis and purification, the low cost of the morpholinium cation source and the possibility of high Li mobility by dissociation of the oxygen group in morpholinium cations. However, although these ILs based on morpholinium cations have characteristics well suited for battery system applications, more improvement on these ILs is required before they are ready for widespread applications in the electrochemical field because of their low ionic conductivities that are caused by melting points higher than room temperature.

In recent years, ILs have been used in electrolyte systems where they play the role of both a charge carrier and nonvolatile plasticizer. These materials were found to exhibit good conductivity and good thermal stability, thus appearing to be potential candidates for use in lithium batteries. With that context, to examine the ionic conductivity of lithium - doped IL electrolytes, we turn back to ILs based on imidazolium cations rather than morpholinium salts. They have already become representative ILs or room temperature ionic liquids (RTILs). Many of them have been well reported, and their synthetic routes and properties are easily accessible. Moreover, they can be commercially purchased from some companies. Two RTILs, 1-butyl-3-methylimidazolium tetrafluoroborate ([BMIm][BF_4]) and 1-butyl-3-methylimidazolium iodide ([BMIm][I]), were synthesized and subsequently lithium salts were doped into these ILs. The physical properties of each IL, such as their reflective indices, densities, viscosities, heat capacities, and heats of dilution, are reported and compared. Ionic conductivities of the lithium-doped systems are investigated as a function of concentration and temperature.

EXPERIMENTAL SECTION

1. Materials

The 1-methylimidazole (99%), 1-chlorobutane (99.5%), 1-iodobutan (99%), ethylacetate, and sodium tetrafluoroborate (98%) were supplied by Aldrich. Dichloromethane and acetonitrile were supplied by KAUTO and MERCK, respectively. All materials were used without any further purification.

2. Synthesis of ILs

2-1. [BMIm][I]

1-Methylimidazole (50 cm^3, 0.627 mol) was dissolved in 500 cm^3 of THF, and 55 cm^3 (0.668 mol) of iodobutane was added to the solution in a 1 L round-bottomed three-necked flask. The mixture was refluxed with vigorous stirring at 323.2 K for 20 h. This brown-colored liquid was isolated and washed with 300 ml of THF. The salt was dried in rotary evaporator and under vacuum for 24 h. The ^1H NMR spectrum (ppm, D_2O) contains the following peaks: δ 8.75 [s, 1H, H(2)], 7.51 [s, 1H, H(4)], 7.46 [s, 1H, H(5)], 4.21 [t, 2H, NCH_2], 3.92 [s, 3H, NCH_3], 1.86 [m, 2H, NCH_2CH_2], 1.34 [m, 2H, $NCH_2CH_2CH_2$], 0.96 [t, 3H, CH_3]. Water content was 15 ppm.

2-2. [BMIm][BF_4]

A 1,000 mL three-necked round-bottomed flask fitted with a water condenser and a gas inlet and provided with a Teflon-coated mag-

†To whom correspondence should be addressed.
E-mail: kks1114@cjnu.ac.kr

netic bar was charged under N_2 with 1-methylimidazole (246.3 g, 3 mol). Butyl chloride (390 mL) was added into the reaction vessel with continuous magnetic stirring in batches of 20 mL. The reaction mixture was heated under nitrogen N_2 at 80 °C for 72 h with stirring until two phases formed. The top phase, containing the unreacted starting material, was decanted and ethyl acetate (300 ml) was added through mixing. The ethyl acetate was decanted followed by the addition of fresh ethyl acetate and this step was repeated twice. After the third decanting of ethyl acetate, any remaining ethyl acetate was removed by heating the bottom phase to 60 °C and stirring while on a vacuum line. The product is slightly yellow and may be crystalline at room temperature, depending on the amount of water present in that phase. The product was recrystallized from dry acetonitrile and dried under vacuum at 70 °C for 12 h to yield pure crystalline [BMIm][Cl]. A solution of [BMIm][Cl] (93 g, 0.531 mol) in acetone (500 cm^3) at room temperature was added to sodium tetrafluoroborate (58.3 g, 0.531 mol). After 24 h stirring, the resulting NaCl precipitate was then filtered through a plug of celite and the volatiles were removed by rotary evaporation to leave a yellowish, clear liquid. The product was dried for three more days under high vacuum at 0.03 mmHg. The chemical shift for the ^{1}H NMR spectrum (ppm, D_2O) appeared as follows: δ 8.71 [s, 1H, H(2)], 7.49 [s, 1H, H(4)], 7.44 [s, 1H, H(5)], 4.21 [t, 2H, NCH_2], 3.91 [s, 3H, NCH_3], 1.87 [m, 2H, NCH_2CH_2], 1.35 [m, 2H, $NCH_2CH_2CH_2$] and 0.94 [t, 3H, CH_3]. The ^{13}C NMR spectrum (ppm, D_2O) contained the following peaks: 137.12 [C(2)], 123.49 [C(4)], 123.12 [C(5)], 50.54 [NCH_2], 36.36 [NCH_3], 32.45 [NCH_2CH_2], 20.06 [$NCH_2CH_2CH_2$] and 13.90 [CH_3]. Water and chloride content was 20 and 13 ppm, respectively.

3. Apparatus and Procedure

3-1. ^{1}H NMR and Cl Anion Contents

The ^{1}H NMR was recorded on a Bruker DMX 600 MHz NMR spectrometer. The possible presence of residual Cl^- was examined by using ionic chromatography (Bio-LC DX-300 (Dionex, Sunnyvale, CA, USA), Detector: Suppressed Conductivity (PED2), Column: ICSep AN300 with ICSep ANSC guard).

3-2. Differential Scanning Calorimeter (DSC)

Thermal analysis and temperature - dependent phase behavior were examined with a Du Pont instrument differential scanning calorimeter (DSC). Samples were loaded in hermetically sealed aluminum pans and measurements were taken over a temperature range of −50 to 100 °C at a heating rate of 10 °C/min under nitrogen atmosphere.

3-2. Conductivity

IL electrolytes were placed between the two stainless steel (SS) electrodes. The ionic conductivities of the electrolyte films were measured by complex impedance analysis with a Solartron 1,260A frequency response analyzer coupled to an IBM computer over a frequency range of 100 Hz-10 MHz. An AC perturbation of 10 mV was applied to the cell. The real and imaginary parts of the complex impedance were plotted, and the ionic conductivity could be calculated from the bulk resistance (Rb) found in the complex impedance diagram.

3-3. Viscosity

The viscosities of the ILs were measured with three appropriate Ubbelohde viscometers. The equipment and procedure used for the viscosity measurement were the same as for our previous investigation [16]. Suitable viscometers were selected considering the viscosity values. The efflux time of the liquid solution through the capillary was measured manually with a stopwatch.

3-4. Density

Two pycnometers were used for the density measurement. The densities of the ILs were calculated from the measured volume and mass values. To determine the volume of the pycnometers at various temperatures (298.2 to 323.2 K, at interval of 5 K), calibration was performed by using triple-distilled water. The volumes of each pycnometer were reproducible within 0.2%. The pycnometers were placed in an air bath to control temperature and measured by a thermometer within ±0.05 K.

3-5. Refractive Index

A precision Abbe refractometer 3T (Atago Co.) was used for the measurement of the refractive index. The entire experimental apparatus consisted of the main measurement unit, a thermosensor for temperature measurement, and a bath circulator. The external bath circulator could control the temperature of the sample droplet within ±0.1 K. Every measurement was performed three times with a reproducibility of $\pm 10^{-4}$.

3-6. Heat of Dilution

The heats of dilution for each IL were measured with an Isoperibol solution calorimeter (CSC4300) from Calorimetric Science Corporation. The calorimeter consisted of a constant temperature bath, a Dewar vessel with a volume of about 25 cm^3, a calibration heater including a 100 Ω resister, a thermister, and a glass stirring rod. The heat of dilution was measured through two phases of operation. Prior to the measurement, the absorbent solution of about 25 cm^3 of the desired concentration was introduced into the Dewar vessel. A small amount of water (about 0.01 g) whose weight was accurately measured was placed in the small cylindrical container. The top and bottom of the cylindrical container were blocked with a fragile cover glass to isolate the inner space of the cylindrical container isolate from the outer space.

The calibration procedures were as follows. The thermister, calibration heater, and stirring rod were immersed after the vessel was clamped on the calorimeter. The stirrer and heater were turned on for heating. The heat was supplied until the solution temperature reached slightly below the desired temperature. With heating for 300 seconds, the actual calibration started through 200 seconds of holding without heating, 400 seconds of heating, and 200 seconds of holding. The amount of heat supplied during the calibration was calculated through measuring the current and voltage values with a built-in digital voltmeter. All procedures were controlled by a connected computer and the measured temperature difference was used to determine the calibration constant in the following equation:

$$Q=(mC_P+\varepsilon)\Delta T \quad (1)$$

where Q is the total amount of heat added, m is the mass of the sample solution, C_P is the heat capacity of the sample in $kJ\cdot kg^{-1}\cdot K^{-1}$, ε is the heat capacity ($kJ\cdot K^{-1}$) of the apparatus, and ΔT is the temperature difference measured by a calorimeter. From the above equation, the heat equivalent E, $mC_p+\varepsilon$, can be determined. The actual measurement of the heat of dilution is similar to the calibration procedure. In this case, the mixing of the solution with water by breaking the cover glass caused the temperature difference. Since we know the heat equivalent, E, from the calibration procedure, the evolved

heat can be calculated from the following equation:

$$H_d=\Delta TE/m_{water} \quad (2)$$

where H_d is the heat of dilution in kJ/kg and m is the weight of water charged in kg. The temperature resolution of the calorimeter was 2 μK, the temperature noise level ±30 mK, and the bath temperature stability ±0.0005 K.

RESULTS AND DISCUSSION

The synthesis procedure of [BMIm][BF_4] was as follows [17-20]:

$$RIm+R'X \rightarrow RR'Im^+X^-$$

where X^- was the tetrafluoroborate anion. The anion exchange using N-butylimidazolium chloride is one of the traditional methods for preparation. In the first step, butylimidazolium chloride was synthesized.

$$RIm+R'X' \rightarrow RR'Im^+X'^-$$

where X' was the chloride anion. Anion exchange reaction was produced by metathesis of the product with the corresponding salts.

$$RIm + R'X' \rightarrow RR'Im^+X'^-$$

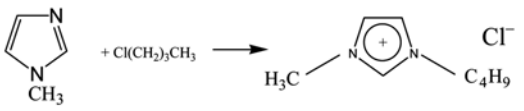

$$RR'Im^+X'^- + MX \rightarrow RR'Im^+X^- + MX'$$

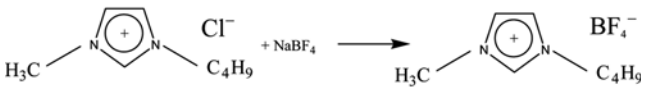

Scheme 1. Synthesis mechanism of [BMIm][BF_4].

Table 1. Physical and electrochemical properties of [BMIm][BF_4]

	T/K					
	298.15	303.15	308.15	313.15	318.15	323.15
r	1.423	1.421	1.420	1.419	1.419	1.417
d/g·cm^{-3}	1.20	1.20	1.19	1.19	1.19	1.18
η/mPa·s	279.86	206.45	147.16	116.64	91.46	72.03
C_p/J·g^{-1}·K^{-1}	1.72	1.75	1.78	1.80	1.83	1.85
H_d/kJ·kg^{-1}				69.5		

Table 2. Physical and electrochemical properties of [BMIm][I]

	T/K					
	298.15	303.15	308.15	313.15	318.15	323.15
r	1.570	1.568	1.567	1.566	1.564	1.561
d/g·cm^{-3}	1.46	1.45	1.45	1.44	1.44	1.44
η/mPa·s	401.24	280.00	195.12	134.35	102.54	80.46

where MX was sodium tetrafluoroborate. Scheme 1 shows the synthesis mechanism of [BMIm][BF_4]. [BMIm][I] was synthesized based on the same synthetic procedure of [BMIm][Cl]. ^{1}H NMR spectra were used for structural analysis of the product. Water and chloride contents were determined with a 756 Karl Fisher coulometer and a Metrohm 716 DMS Titrino, respectively. The records on the impurity contents in ILs are important because the various properties of ILs strongly depend on the halogen anion and water contents.

The physical properties of [BMIm][BF_4] and [BMIm][I] are summarized in Table 1 and Table 2, respectively [2,3]. The density values decrease, but the heat capacities increase with increasing temperature. The temperature effect on refractive index appears to be almost negligible. Density and refractive index values of [BMIm][I] are higher than those of [BMIm][BF_4]. In the case of viscosity measurement, [BMIm][I] is more viscous than [BMIm][BF_4]. The overall properties of [BMIm][BF_4] were superior to those of the IL with the halide anion.

Twelve samples for which the compositions ranged between 0 and 50 mol% $LiBF_4$ were prepared for conductivity measurements. Ionic conductivities of all samples were determined with a Solartron 1260A frequency response analyzer (FRA) in the temperature range from 298.15 to 323.15 K. The ionic conductivities of neat [BMIm][BF_4] and [BMIm][I] were also measured over the same temperature range in order to compare the conductivities of Li-doped ILs. Fig. 1 shows ionic conductivities for Li-doped [BMIm][BF_4] as a function of temperature. The neat [BMIm][BF_4] showed ionic conductivities of 10^{-4} S·cm^{-1}. Ionic conductivities increased with increasing temperature, while they reached maximum values at an optimal concentration between 30 and 40 mol% $LiBF_4$, as shown in Fig. 2. The values were 10^{-3} order at temperatures from 308.15 K to 323.15 K. The increase in the thermal motion of ions as a

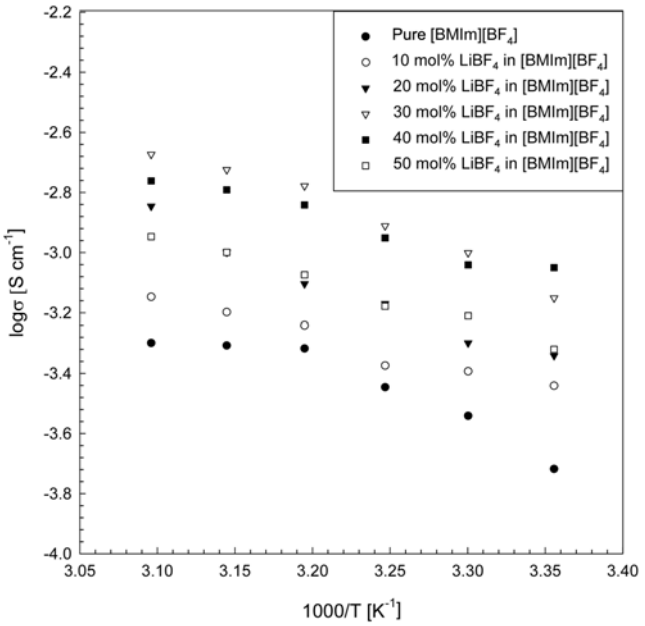

Fig. 1. Ionic conductivities for lithium doped [BMIm][BF_4] (conductivity vs. temperature).

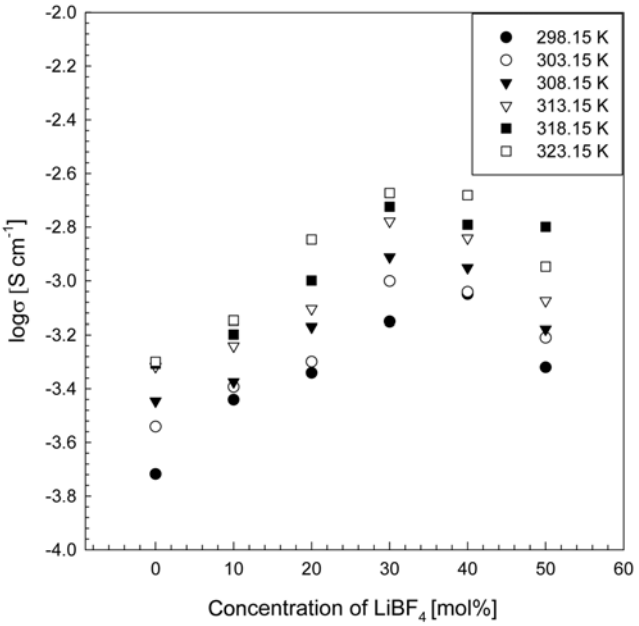

Fig. 2. Ionic conductivities for lithium doped [BMIm][BF$_4$] (conductivity vs. LiBF$_4$ concentration).

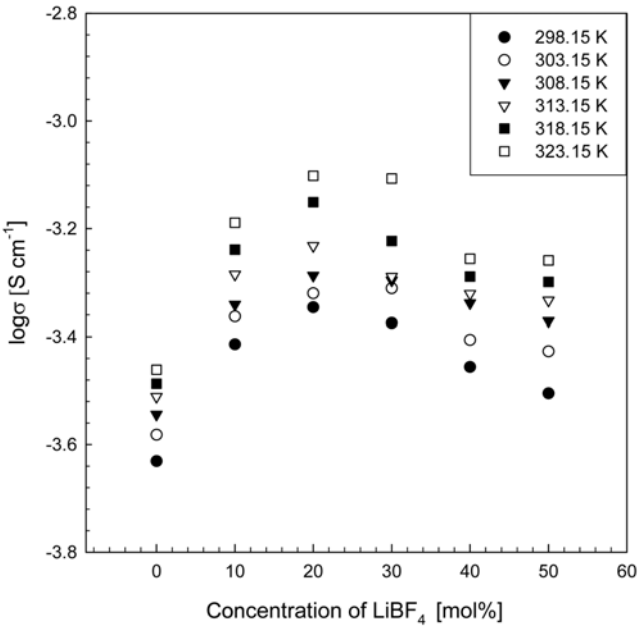

Fig. 4. Ionic conductivities for lithium doped [BMIm][I] (conductivity vs. LiBF$_4$ concentration).

function of temperature causes a rapid improvement in the conductivity. The isotherm data in Fig. 2 show the parabolic curves, indicating a specific concentration of $LiBF_4$ exists corresponding to a maximum conductivity value between 30 and 40 mol%. Doping with up to 30 or 40 mol% of $LiBF_4$ produces a gradual increase in conductivity. The phenomena of ionic conduction are attributed to increases in effective carrier ion density and its mobility as the concentration of Li ions increases. In contrast, beyond the concentration of 30 or 40 mol% of $LiBF_4$ the conductivity begins to fall. It appears that the complex ion interaction at high concentrations between each cation and anion not only interferes with the ion conduction but also increases the viscosity of the system.

The same tendency for the Li-doped [BMIm][I] electrolytes was observed and the same interpretation can be applied. All ionic conductivities stayed at 10^{-4} order, as shown in Fig. 3, indicating that they are less than the ionic conductivities in Li-doped [BMIm][BF_4] systems. It is reasonable considering the higher viscosity of [BMIm][I] compared to the viscosity of [BMIm][BF_4]. Fig. 4 shows the maximum points of the parabolic curves are at between 20 and 30 mol%.

Figs. 5 and 6 display preliminary data of the Li NMR for the suggested systems in order to ascertain whether or not the conductivity of lithium increases. It has been well explained that Li NMR linewidth data as a function of temperature indirectly reflect the mobil-

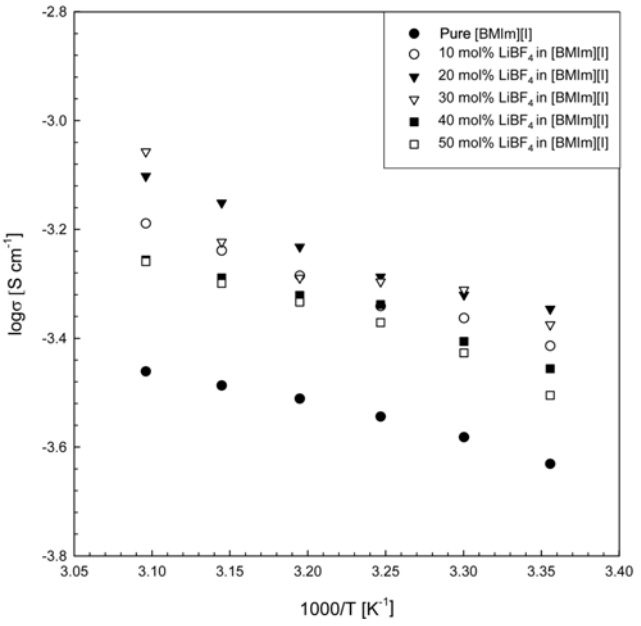

Fig. 3. Ionic conductivities for lithium doped [BMIm][I] (conductivity vs. temperature).

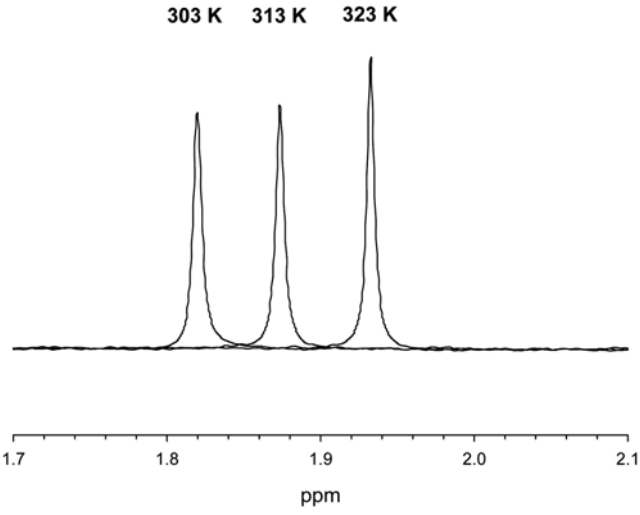

Fig. 5. Li-NMR spectrum of 30 mol% LiBF$_4$ in [BMIm][BF$_4$].

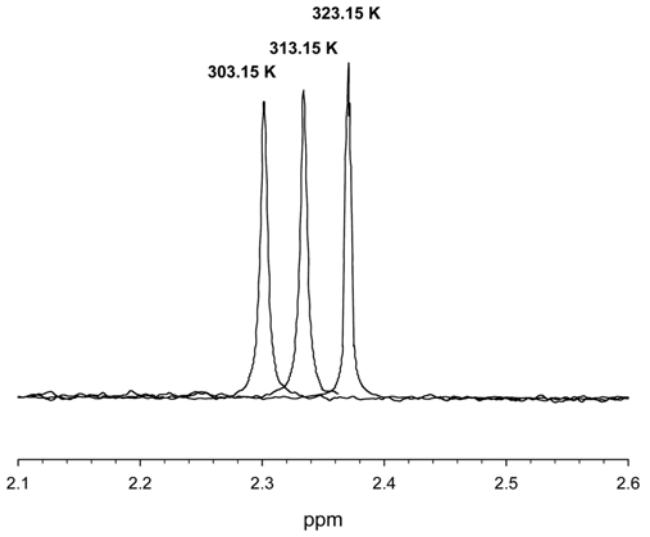

Fig. 6. Li-NMR spectrum of 30mol% $LiBF_4$ in [BMIm][I].

ity of lithium [4-9]. The width of the Li resonance as a function of temperature can be a probe to observe the diffusive motions of Li ions. Generally, with increasing temperature, the diffusive motions cause a narrow linewidth. Temperature-dependent Li NMR spectra for two samples containing 30 mol% $LiBF_4$ at 303.15, 313.15, and 323.15 K are presented in Figs. 5 and 6. Although both linewidths at 323.15 K in Figs. 5 and 6 appeared to become narrower, all peaks at three temperatures show similar shapes because no thermal transitions such as solid-solid and solid-liquid transitions took place in the temperature range. The NMR measurement therefore does not offer conclusive proof of lithium ion motion over the given temperature range. The measurement range in temperature and Li concentration should be extended in order to more exactly interpret the conductivity phenomena of the Li ion itself in the matrix.

CONCLUSION

Two ILs, [BMIm][BF_4] and [BMIm][I], were selected in order to investigate the ion conductivities for Li-doped IL systems. The physical properties of [BMIm][BF_4] and [BMIm][I] were examined and compared. The highest conductivities of the Li-doped [BMIm][BF_4] system were between 30 and 40 mol% $LiBF_4$, whereas the highest values of the Li-doped [BMIm][I] system were between 20 and 30 mol% $LiBF_4$. Conductivity in these doped systems is very significantly higher than for the pure ILs.

ACKNOWLEDGMENT

This work was supported by the Korea Research Foundation Grant funded by the Korean Government (KRF-2008-331-D00110). I am grateful to KBSI (Korea Basic Science Institute) for assistance with NMR, FAB mass, and ion chromatography.

NOMENCLATURE

d	: density
η	: viscosity
r	: refractive index
C_p	: heat capacity [$kJ \cdot kg^{-1} \cdot K^{-1}$]
ε	: heat capacity of the apparatus [$kJ \cdot K^{-1}$]
H_d	: heat of dilution
Q	: heat [kJ]
δ	: chemical shift in NMR
T	: temperature, K
σ	: conductivity
IL	: ionic liquid

REFERENCES

1. K. N. Marsh, A. Deev, A. C.-T. Wu, E. Tran and A. Klamt, *Korean J. Chem. Eng*., **19**, 357 (2002).
2. K.-S. Kim, B.-K. Shin, H. Lee and F. Ziegler, *Fluid Phase Equilibria*, **218**, 215 (2004).
3. K.-S. Kim, B.-K. Shin and H. Lee, *Korean J. Chem. Eng*., **21**, 1010 (2004).
4. D. R. MacFarlane, J. Huang and M. Forsyth, *Nature*, **402**, 792 (1999).
5. D. R. MacFarlane and M. Forsyth, *Adv. Mater.*, **13**, 957 (2001).
6. M. Forsyth, J. Huang and D. R. MacFarlane, *J. Mater. Chem.*, **10**, 2259 (2000).
7. D. R. MacFarlane, P. Meakin, J. Sun, N. Amini and M. Forsyth, *J. Phys. Chem. B*., **103**, 4164 (1999).
8. D. R. McFarlane, J. Sun, J. Golding, P. Meakin and M. Forsyth, *Electrochim. Acta*., **45**, 1271 (2000).
9. S. Forsyth, J. Golding, D. R. MacFarlane, M. Forsyth, *Electrochim. Acta*., **46**, 1753 (2001).
10. J. Fuller, Amy C. Breda and Richard T. Carlin, *J. Electroanal. Chem.*, 495 (1998).
11. K.-S. Kim, S. Choi, D. Demberelnyamba, H. Lee, J. Oh, B.-B. Lee and S.-J. Mun, *Chem. Commun*., 828 (2004).
12. K.-S. Kim, S.-Y. Park, S.-H. Yeon and H. Lee, *Electrochimica Acta.*, **50**, 5673 (2005).
13. K.-S. Kim, S.-Y. Park, S. Choi and H. Lee, *J. Power Sources*, **155**, 385 (2006).
14. S. Choi, K.-S. Kim, H. Lee, J. S. Oh and B. B. Lee, *Korean J. Chem. Eng*., **22**, 281 (2005).
15. J.-H. Cha, K.-S. Kim, S. Choi, S.-H. Yeon, H. Lee, H. S. Kim and H. Kim, *Korean J. Chem. Eng*., **22**, 945 (2005).
16. K.-S. Kim and H. Lee, *J. Chem. Eng. Data*, **47**, 216 (2002).
17. R. Hagiwara and Y. Ito, *J. Fluorine Chem.* **105**, 221 (2000).
18. P. Bonhote, A.-P. Dias, N. Papageorgiou, K. Kalyanasundaram and Gratzel. M. Hydrophobic, *Inorg. Chem*. **35**, 1168 (1996).
19. P. A. Z. Suarez, J. E. L. Dullius, S. Einloft, R. F. D. Souza and J. Dupont, *Polyhedron*, **15**, 1217 (1995).
20. F.-D. Joan and P. B. Jean, *Tetrahedron Letter*, **42**, 6097 (2001).